Contribution from the Department of Chemistry,
University of Houston, Houston, Texas 77004

Reactions of Metalloporphyrin π Radicals. 3. Solvent- and Ligand-Binding Effects on the One-Electron Oxidation of 5,10,15,20-Tetraphenylporphyrin d^{10} Metal Ions in Nonaqueous Media

K. M. KADISH* and L. R. SHIUE

Received March 4, 1982

Stability constants for nitrogenous base addition to $(TPP)M^{II}$ and $[(TPP)M^{II}]^+$ were determined where M = Cd and Hg. Spectrophotometric methods were utilized for the determination of the five-coordinate neutral complexes (TPP)M(L) and comparisons made with earlier published values of (TPP)Zn(L) formation. For formation of (TPP)Hg(L) values of log β_1^0 ranged from 0.25 to 4.34. Larger values were obtained for formation of (TPP)Cd(L). Positive correlations were obtained from plots of log β_1^0 vs. the ligand pK_a, indicating the complexations were dominated by σ-bond strength of the ligand. Reversible half-wave potentials of the $(TPP)M(L)/[(TPP)M(L)]^+$ couple shifted in a cathodic or an anodic direction by −140 to +70 mV from that of $(TPP)M/[(TPP)M]^+$ depending upon the bound ligand. Similar shifts in potential were seen upon changing from a nonbonding nonaqueous solvent to a bonding one. Values of log β_1^0 were combined with electrochemical data to obtain stability constants (log β_1^+) for the complexation of $[(TPP)M]^+$ with nitrogenous bases. Linear relationships with positive slopes were also seen for the correlation of log β_1^+ with pK_a of the substituted pyridines. Finally, comparisons were made between the spectral properties and reactivity of each (TPP)M(L) series.

Introduction

Recently our laboratory has begun to reinvestigate the electrochemical reactivity of metalloporphyrin radical cations and radical anions in nonaqueous media.[1-3] Our aim was to interpret the shifts of potential for oxidation or reduction of the complexes as well as changes in electron-transfer mechanisms in terms of the axial ligand binding properties of the oxidized *and* reduced forms of the complex. It is quite evident that standard potentials of porphyrins must be interpreted in terms of both the oxidized and reduced forms of the complex and that structure–reactivity relationships of a single oxidation state are not sufficient to define how potentials or mechanisms of redox processes may be modified. Previous studies from several laboratories[3-9] concentrated on measuring stability constants for porphyrin complexes containing metals of +3, +2 or +1 oxidation states which could be coupled in the redox reaction M(III)/M(II) or M(II)/M(I). However, most of these studies examined only the complexes of Fe, Mn, and Co, and in no cases did the complexes contain a charged porphyrin ring as one form of the redox couple.

Thirty years ago Miller and Dorough[10] measured stability constants for addition of pyridine to tetraphenylporphyrin complexes of Zn, Cd, and Hg, as well as Mg and Cu. For the reaction

$$(TPP)M + L \rightleftarrows (TPP)M(L) \qquad (1)$$

values of log β_1 were 3.79, 3.58, and 1.22 where M = Zn, Cd, and Hg, respectively. Similar values were obtained for pyridine addition to Zn, Cd, and Hg porphyrin complexes by Kirksey and Hambright[11] 18 years later. In addition, four other substituted pyridines were investigated as donor ligands in that study and linear free energy relationships described between log β_1 for reaction 1 and the ligand pK_a or the σ of the substituted pyridine.

Both the study by Miller and Dorough and that by Kirksey and Hambright were carried out at zero ionic strength. In this present study, measurements of stability constants for the neutral complexes were made in solvents containing 0.1 M TBAP so that a direct comparison could be made between the electrochemical and spectral studies of the reactant and product.

Because porphyrin complexes of Zn(II) have been well-characterized in the literature as to their ligand-binding properties[11-16] and because their electrochemical reactivity is well-defined,[17-20] we had selected these complexes for our initial study of radical-binding reactions.[1-3] In all cases only five-coordinate nitrogenous base adducts of $[(TPP)Zn]^+$ could be observed in CH_2Cl_2 and formation constants were calculated for conversion of $[(TPP)Zn]^+$ to $[(TPP)Zn(L)]^+$ where L was one of 20 different nitrogenous bases.[1] This present paper is a continuation of our initial study and involves the electrochemistry of (TPP)Cd, $[(TPP)Cd]^+$, (TPP)Hg, and $[(TPP)Hg]^+$ with the same 20 nitrogenous bases as utilized for reactions with (TPP)Zn and $[(TPP)Zn]^+$. In addition, we have also investigated these complexes in the presence of 12 nonaqueous solvents, some of which could act as donor ligands. These d^{10} complexes of metalloporphyrins are ideal for this study in that they form only five-coordinate species in nonaqueous media and that they also have readily accessible oxidation potentials within the range of most electrochemical solvents.

The electrochemical oxidation of (TPP)Zn and (TPP)Cd has been well studied in nonaqueous media.[17,18] Electrochemical oxidation reversibly yields first a π cation radical and then a dication according to the reactions

$$(TPP)M \overset{-e^-}{\rightleftharpoons} [(TPP)M]^+ \qquad (2)$$

$$[(TPP)M]^+ \overset{-e^-}{\rightleftharpoons} [(TPP)M]^{2+} \qquad (3)$$

(1) Kadish, K. M.; Shiue, L. R.; Rhodes, R. K.; Bottomley, L. A. *Inorg. Chem.* **1981**, *20*, 1274.
(2) Kadish, K. M.; Rhodes, R. K. *Inorg. Chem.* **1981**, *20*, 2961.
(3) Kadish, K. M.; Bottomley, L. A.; Kelly, S.; Schaeper, D.; Shiue, L. R. *Bioelectrochem. Bioenerg.* **1981**, *8*, 213.
(4) Kadish, K. M.; Bottomley, L. A.; Beroiz, D. *Inorg. Chem.* **1978**, *17*, 1124.
(5) Truxillo, L. A.; Davis, D. G. *Anal. Chem.* **1975**, *47*, 2260.
(6) Manassen, J. *Isr. J. Chem.* **1974**, *12*, 1059.
(7) Lexa, D.; Momenteau, M.; Mispelter, J.; Lhoste, J. M. *Bioelectrochem. Bioenerg.* **1974**, *1*, 108.
(8) Kadish, K. M.; Kelly, S. *Inorg. Chem.* **1979**, *18*, 2968.
(9) Kadish, K. M.; Bottomley, L. A. *Inorg. Chem.* **1980**, *19*, 832.
(10) Miller, J. R.; Dorough, G. D. *J. Am. Chem. Soc.* **1952**, *74*, 3977.
(11) Kirksey, C. H.; Hambright, P. *Inorg. Chem.* **1970**, *9*, 958.
(12) Kirksey, C. H.; Hambright, P.; Storm, C. B. *Inorg. Chem.* **1969**, *8*, 2141.
(13) Nappa, M.; Valentine, J. S. *J. Am. Chem. Soc.* **1978**, *100*, 5075.
(14) Grant, C., Jr.; Hambright, P. *J. Am. Chem. Soc.* **1969**, *91*, 4195.
(15) Vogel, G. C.; Searby, L. A. *Inorg. Chem.* **1973**, *12*, 936.
(16) Cole, S. J.; Curthoys, G. C.; Magnusson, E. A.; Phillips, J. N. *Inorg. Chem.* **1972**, *11*, 1024.
(17) Stanienda, A.; Biebl, G. *Z. Phys. Chem. (Wiesbaden)* **1967**, *52*, 254.
(18) Lexa, D.; Reix, M. *J. Chim. Physiochim. Biol.* **1974**, *71*, 511.
(19) Lanse, J. G.; Curthoys, G. S. *J. Electrochem. Soc.* **1972**, *119*, 1039.
(20) Felton, R. H.; Linschitz, H. *J. Am. Chem. Soc.* **1966**, *88*, 1113.

0020-1669/82/1321-3623$01.25/0

Table I. Stability Constants (log β_1^0) for Axial Ligand Addition of Nitrogenous Bases to (TPP)M in Nonbonding Solvents

			(TPP)Zn		(TPP)Cd		(TPP)Hg	
no.	ligand	pK_a[a]	lit.[b]	lit.[c]	this work[d]	lit.[e]	this work[f]	lit.[e]
1	3,5-dichloropyridine	0.67	2.50		1.72		[g]	
2	3-cyanopyridine	1.45	2.70	2.80 ± 0.04	1.98		[g]	
3	4-cyanopyridine	1.86	2.84	2.9 ± 0.1	2.21	2.27	0.25	0.22
4	3-chloropyridine	2.81	3.00		2.44		0.42[h]	
5	3-bromopyridine	2.84	3.06		2.53		0.51	
6	3-acetylpyridine	3.18	3.19		2.68		0.59	
7	4-acetylpyridine	3.51	3.27		2.89		0.74	
8	pyridine	5.29	3.62	3.78 ± 0.02	3.37	3.51	1.45	1.21
9	3-picoline	5.79	3.76	3.82 ± 0.07	3.54		1.67	1.41
10	2-picoline	5.96	2.25	2.30 ± 0.04	3.62		1.76	
11	4-picoline	5.98	3.82	4.02 ± 0.05	3.70	3.83	1.74	1.62
12	3,4-lutidine	6.46	3.98		3.85		2.00	
13	2-aminopyridine	6.82	2.76		3.91		2.16	
14	4-aminopyridine	9.17	4.49	4.65 ± 0.04	4.81	4.73	2.96	2.92
15	4-(*N,N*-dimethylamino)pyridine	9.71	4.61		5.04		4.04	
16	piperidine	11.1	4.90	5.05 ± 0.05	5.34		4.34	
17	imidazole	6.65	5.11		4.23		2.73[i]	
18	1-methylimidazole	7.33	5.16		5.03		2.82	
19	2-methylimidazole	7.56	5.32		5.30		3.04	
20	1,2-dimethylimidazole	7.85	5.47		5.59		3.20	

[a] Schoefield, K. S. "Hetero-Aromatic Nitrogen Compounds"; Plenum Press: New York, 1967; p 146. [b] Reference 1; in CH_2Cl_2-0.1 M TBAP; deviation ±0.03 for ligands **1-16** and ±0.06 for ligands **17-20**. [c] Reference 12; in benzene. [d] In $CHCl_3$-0.1 M TBAP; deviation ±0.06 for ligands **1-16** and ±0.08 for ligands **17-20**. [e] Reference 11; deviation ± 0.05. [f] In $CHCl_3$-0.1 M TBAP; deviation ±0.03 for ligands **1-16** and ±0.05 for ligands **18-20** and 0.15 for ligand **17**. [g] Stability is constant less than 0.25. [h] Uncharacterized reaction of (TPP)Hg(3-Clpy) occurs when ligand concentration is >1.0 M. This reaction is not a demetalation. [i] Rapid demetalation occurs after formation of (TPP)Hg(Im). Only about 100 data points were utilized in the SQUAD calculations, which can evaluate stability constants at low ligand/porphyrin ratios.

No reports of (TPP)Hg electrochemistry have appeared in the literature, but this complex also undergoes the preceding two electrooxidations.

As already mentioned, we have completed investigations of (TPP)Zn oxidation in the presence and absence of nitrogenous bases.[1-3] Cyclic voltammetry and thin-layer spectra indicate that the first oxidation of ligated (TPP)Zn is electrochemically and spectrally reversible.[2] However, the mechanism for the second oxidation involves coupled chemical reactions. Similar follow-up chemical reactions are also observed after formation of the dications of $[(TPP)Cd(L)]^{2+}$ and $[(TPP)Hg(L)]^{2+}$. For this reason, we are only concerned in this paper with reactions of the cation radical, which is well defined-both chemically and electrochemically.

Experimental Section

Chemicals. The synthesis and purification of (TPP)Zn have been described in a previous work.[1,2] (TPP)Cd was prepared by the method of Rodesiler et al.[21] and purified by chromatography on a column of basic alumina. (TPP)Hg was synthesized following the method of Hudson and Smith.[22] After recrystallization from methylene chloride and hexane, chromatography was not possible with (TPP)Hg because of decomposition on the chromatography column.[23] All synthesized metalloporphyrins had the same optical absorption spectra as reported in the literature.[24,27]

Purification of the electrochemical solvent, methylene chloride (CH_2Cl_2), the supporting electrolyte, tetrabutylammonium perchlorate (TBAP), and the substituted pyridines and imidazoles used as ligands has been reported in previous publications.[1,2] Due to the limited solubility of (TPP)Cd and (TPP)Hg in CH_2Cl_2, chloroform ($CHCl_3$) was employed as the solvent for preparing stock solutions of these complexes for use in the spectrophotometric measurements. Spectrophotometric grade $CHCl_3$ was obtained from Aldrich and was passed through an alumina column to remove any existed ethanol. The other nonaqueous solvents utilized in the study were purified by literature methods.[25]

Instrumentation. Most optical absorption measurements were made on a Cary 14 spectrophotometer. However, as has been pointed out by several laboratories,[26,27] solutions containing Cd or Hg tetraphenylporphyrins gradually deteriorate upon exposure to light. So that decomposition could be avoided as much as possible, porphyrin solutions were prepared fresh before each spectrophotometric measurement. In this study, (TPP)Hg also showed demetalation on mixing with several nitrogenous bases. For bases that caused fast demetalation with (TPP)Hg, a Tracor Northern 1710 holographic optical spectrometer/multichannel analyzer was used, with spectra taken as soon as possible after addition of ligands to the porphyrin solutions.[28] With the TN 1710, spectra result from the signal averaging of 100 sequential 5-ms spectral acquisitions. Each acquisition represents a single spectrum from 325 to 952 nm, simultaneously recorded by a diode-array detector with a resolution of 1.2 nm/channel.

Cyclic voltammetric measurements were made with an EG&G Princeton Applied Research (PAR) Model 174 polarographic analyzer in conjunction with a Houston Omnigraphic 2000 X-Y recorder at scan rates of 0.020–0.500 V/s. A three-electrode system, consisting of a Pt-button working electrode, a Pt-wire counterelectrode, and a commercial saturated calomel electrode (SCE), was utilized. Details of the instrumentation have been presented in previous publications.[1-3]

Data Treatment. Stability constants (log β_1^0) for the axial ligand addition of nitrogenous bases to (TPP)Cd and (TPP)Hg were initially calculated by using Benesi-Hildebrand plots. These determinations for log β_1^0 were then modified by using a computer program, SQUAD, which has been described in a previous study of (TPP)Mg complexation.[29]

Stability constants (log β_1^+) for the complexation of $[(TPP)Cd]^+$ and $[(TPP)Hg]^+$ π radical cations with nitrogenous bases were de-

(21) Rodesiler, P. F.; Griffith, E. H.; Ellis, P. D.; Amma, E. L. *J. Chem. Soc., Chem. Commun.* **1980**, 492.
(22) Hudson, M. F.; Smith, K. M. *Tetrahedron* **1976**, 597.
(23) Davis, B. A.; Hui, K. S.; Durden, D. A.; Boulton, A. A. *Biomed. Mass Spectrom.* **1976**, *3*, 71.
(24) Hudson, M. F.; Smith, K. M. *Tetrahedron Lett.* **1974**, 2227.
(25) Perrin, D. D.; Armarego, W. L. F.; Perrin, D. R. "Purification of Laboratory Chemicals", 2nd ed.; Pergamon Press: New York, 1980.
(26) Storm, C. G.; Corwin, A. H.; Arellano, R. R.; Martz, M.; Weintraub, R. *J. Am. Chem. Soc.* **1966**, *88*, 2525.
(27) Dorough, G. D.; Miller, J. R.; Huennekens, F. J. *J. Am. Chem. Soc.* **1951**, *73*, 4315.

(28) Titrations of (TPP)Hg with all nitrogenous bases showed five-coordinate complexes were rapidly formed at low ligand concentrations. Under these conditions stability constants could be obtained without demetalation, which was sometimes observed at higher values of ligand concentration. This most often involved complexation with imidazoles and will be the subject of a future communication.

(29) Kadish, K. M.; Shiue, L. R. *Inorg. Chem.* **1982**, *21*, 1112.

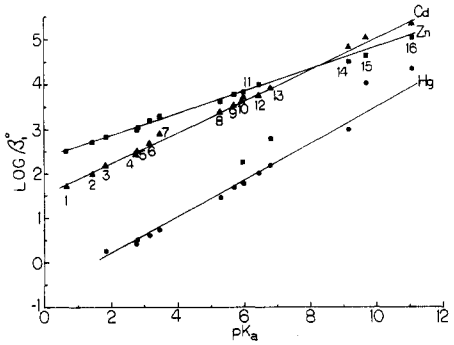

Figure 1. log β_1^0 vs. ligand pK_a for (TPP)M(L), where M = Zn (■), Cd (▲), and Hg (●).

Table II. Effect of pK_a of Axially Bound Ligand on Stability Constants for (TPP)M(L) and [(TPP)M(L)]$^+$ according to Eq 5

complex	stability const considered	ligands included[a]	slope (a)	intercept (b)	correl coeff
(TPP)Zn(L)	β_1^0	1-9, 12, 14-16	0.23	2.41	0.998
[(TPP)Zn(L)]$^+$	β_1^+	1-9, 11, 12	0.49	1.40	0.992
(TPP)Cd(L)	β_1^0	1-16	0.36	1.52	0.998
[(TPP)Cd(L)]$^+$	β_1^+	2-12	0.51	−0.24	0.987
(TPP)Hg(L)	β_1^0	3-16	0.46	−0.86	0.988
[(TPP)Hg(L)]$^+$	β_1^+	4-11	0.61	−0.82	0.992

[a] See Table I for identity of ligands.

termined by monitoring the shifts in $E_{1/2}$ as a function of free-ligand concentration, [L]. Plots of $E_{1/2}$ vs. log [L] were constructed, and from the slope of the plots, the change in axial ligand coordination number was determined by eq 4, where $(E_{1/2})_c$ and $(E_{1/2})_s$ are the

$$(E_{1/2})_c = (E_{1/2})_s - (0.059/n) \log (\beta_1^+/\beta_1^0) - (0.059/n) \log [L]^{p-q} \quad (4)$$

half-wave potentials of the complexed species and uncomplexed species, respectively, [L] is the free-ligand concentration, n is the number of electrons transferred in the diffusion-controlled reaction, and p and q are the number of ligands bound to the cation radical and neutral species, respectively. For each ligand β_1^0 was determined spectrophotometrically and combined with the electrochemical data to calculate values for β_1^+ at 1 M ligand.

Results

log β_1^0 values for addition of 20 different nitrogenous bases to (TPP)Cd and (TPP)Hg, together with available literature values, are listed in Table I. The values calculated in this work are in good agreement with published literature values. Also included in Table I are data already published for ligand addition to (TPP)Zn.[2,11,12] For a given ligand the magnitude of log β_1^0 generally decreases in the order Zn > Cd > Hg, which is consistent with the trend observed by other investigators.[11] There is, however, a crossover of this trend with ligands of higher pK_a where log β_1^0 for (TPP)Cd is slightly greater than for (TPP)Zn. This is best illustrated in Figure 1, which shows the correlation between log β_1^0 and the pK_a of the substituted pyridines.

In terms of hard and soft acids, or class a and class b acids, Zn(II) is a borderline Lewis acid, while Cd(II) and Hg(II) are class b acids. Each constant is a linear function of the ligand pK_a, as indicated by the linear regression fit listed in Table II. Every correlation is a function of the form

$$\log \beta_1^0 = apK_a + b \quad (5)$$

where a is the slope and b is the intercept.

It has been suggested that a is related to the σ polarizability of a cation,[11] and a successful correlation of the measured properties with the ligand characteristics such as pK_a and donor number implies that σ-bond strength considerations dominate the trends in the measured properties.

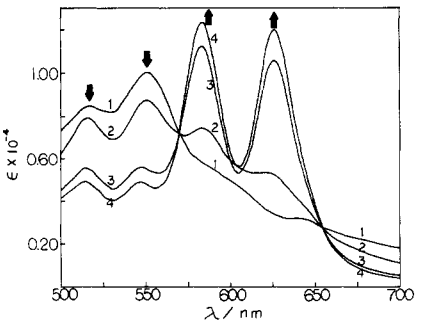

Figure 2. Optical absorption spectra obtained during spectrophotometric titration of 5×10^{-5} M (TPP)Hg–0.1 M TBAP in $CHCl_3$ with 3-picoline. Mole ratio of ligand to porphyrin: (1) 0/1; (2) 100/1; (3) 2000/1; (4) 18000/1.

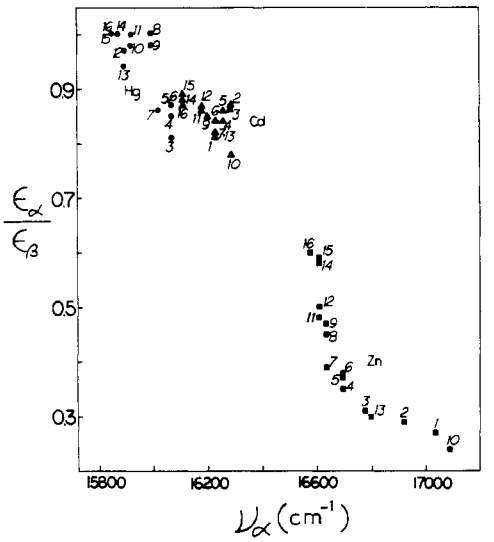

Figure 3. Plot of $\epsilon_\alpha/\epsilon_\beta$ vs. the α-band frequency (ν_α) for (TPP)M(L) derivatives where M = Cd (▲), Hg (●), and Zn (■). Numbers correspond to ligands in Table I.

Generally, upon insertion of a metal into $TPPH_2$ the four visible bands of the free base will be replaced by two, the so-called α and β bands. It is noted (Figure 2) that completely formed α and β bands are not present with (TPP)Hg. Upon addition of ligand, however, well-defined α and β bands do appear as illustrated by the titration of (TPP)Hg with 3-picoline, which is shown in Figure 2. Addition of a fifth axial ligand will then result in a shift of wavelength and change of intensity of the two visible peaks as a function of the strength and type of axial ligand interaction. This is shown in Table III, which lists the absorption maxima and molar absorptivities for the main peaks of (TPP)Cd(L), (TPP)Hg(L), and (TPP)Zn(L). As seen from this table, large bathochromic shifts are seen on adding a fifth ligand to the four-coordinate complex.

Numerous correlations between the spectral properties in Table III and donor properties of the bound ligand on (TPP)M(L) were attempted. Two of these correlations are given in Figures 3 and 4. Figure 3 illustrates the relationship between the ratio of the α and β band molar absorptivities ($\epsilon_\alpha/\epsilon_\beta$) and the position of the α band. A similar plot gave linear correlations for (TPP)Zn(L) with a variety of different neutral and negatively charged donor ligands.[13] In Figure 4 we have plotted the same ratio of molar absorptivities, $\epsilon_\alpha/\epsilon_\beta$, vs. the experimentally obtained formation constant for ligand addition according to eq 1. Values of log β_1^0 are taken from the data in Table I.

Table III. Absorption Maxima (in nm) of the Main Peaks of (TPP)M and (TPP)M(L) with Molar Absorptivities ($\epsilon \times 10^{-4}$) Given in Parentheses

	Zn				Cd				Hg			
ligand[a]	Soret	α	β	$\epsilon_\alpha/\epsilon_\beta$	Soret	α	β	$\epsilon_\alpha/\epsilon_\beta$	Soret	α	β	$\epsilon_\alpha/\epsilon_\beta$
none	419 (56.5)	585 (0.49)	547 (2.34)	0.21	430 (42.2)	602 (0.85)	562 (1.56)	0.54	429 (45.8)	*b*	*b*	
1	420 (51.2)	587 (0.55)	548 (2.04)	0.27	436 (46.2)	614 (1.02)	572 (1.31)	0.78	*c*	*c*	*c*	
2		591 (0.57)	549 (1.96)	0.29		614 (1.29)	572 (1.48)	0.87		*c*	*c*	
3		596 (0.57)	549 (1.87)	0.31		614 (1.21)	572 (1.40)	0.86		622 (0.76)	581 (0.93)	0.82
4	426 (54.4)	599 (0.62)	551 (1.79)	0.35	436 (46.8)	615 (1.17)	573 (1.39)	0.84	435 (40.6)[d]	622 (0.88)	580 (1.03)	0.85
5		599 (0.64)	551 (1.74)	0.37		615 (1.21)	573 (1.41)	0.86		622 (0.94)	581 (1.08)	0.87
6		599 (0.64)	551 (1.70)	0.38		616 (1.32)	574 (1.57)	0.84		622 (0.99)	582 (1.14)	0.87
7		601 (0.65)	553 (1.66)	0.39		616 (1.26)	574 (1.53)	0.82		624 (1.02)	584 (1.19)	0.86
8	428 (53.8)	601 (0.76)	561 (1.68)	0.45	427 (46.6)	616 (1.24)	575 (1.49)	0.83	436 (46.0)	626 (1.26)	585 (1.25)	1.01
9		601 (0.82)	561 (1.76)	0.47		617 (1.29)	575 (1.52)	0.85		626 (1.28)	583 (1.31)	0.98
10		585 (0.49)	548 (2.08)	0.24		616 (1.28)	574 (1.58)	0.81		628 (1.29)	585 (1.32)	0.98
11		602 (0.85)	562 (1.76)	0.48		618 (1.20)	576 (1.40)	0.86		628 (1.23)	585 (1.23)	1.00
12	428 (55.7)	602 (0.40)	562 (1.79)	0.50	437 (45.8)	618 (1.37)	576 (1.58)	0.87	438 (41.2)	629 (1.32)	585 (1.36)	0.97
13		595 (0.55)	550 (1.83)	0.30		616 (1.22)	575 (1.46)	0.82		629 (1.29)	586 (1.37)	0.94
14		602 (1.08)	562 (1.87)	0.58		619 (1.40)	576 (1.60)	0.88		630 (1.33)	587 (1.30)	1.02
15		602 (1.18)	562 (1.83)	0.59		619 (1.23)	576 (1.40)	0.89		631 (1.31)	587 (1.29)	1.02
16	429 (57.6)	603 (1.17)	563 (1.96)	0.60	437 (46.6)	619 (1.30)	576 (1.49)	0.87	443 (43.0)	631 (1.28)	588 (1.21)	1.06
17	428 (58.4)	602 (1.13)	562 (1.81)	0.62	437 (48.6)	619 (1.13)	576 (1.26)	0.90	*e*	*e*	*e*	*e*
18	429 (58.1)	603 (1.22)	563 (2.02)	0.60	438 (48.8)	620 (1.37)	578 (1.58)	0.87	439 (44.0)	630 (1.27)	588 (1.33)	0.96
19		603 (1.17)	563 (1.98)	0.59		619 (1.08)	577 (1.24)	0.87		631 (0.98)	588 (1.02)	0.96
20		604 (1.11)	564 (1.89)	0.59		620 (1.59)	578 (1.38)	1.15		631 (1.37)	588 (1.36)	1.01

[a] Ligand is identified in Table I. [b] See Figure 2. [c] Complete spectra of (TPP)Hg(L) not formed even at the highest ligand concentration. [d] Uncharacterized reaction of (TPP)Hg(3-Clpy) occurs when ligand concentration is >1.0 M. This reaction is not a demetalation. [e] Rapid demetalation occurs after formation of (TPP)Hg(Im).

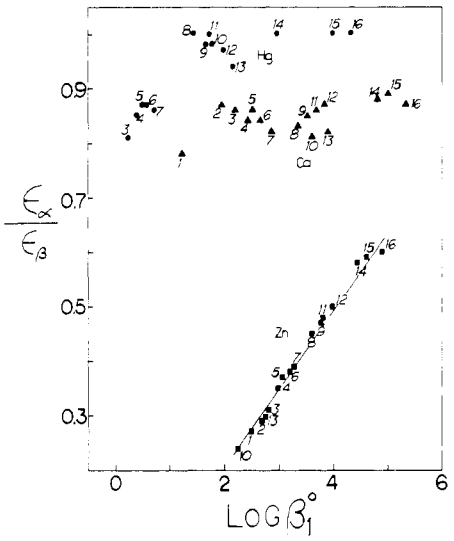

Figure 4. Plot of $\epsilon_\alpha/\epsilon_\beta$ vs. log β_1^0 for formation of (TPP)M(L) where M = Cd (▲), Hg (●), and Zn (■). Numbers correspond to ligands in Table I.

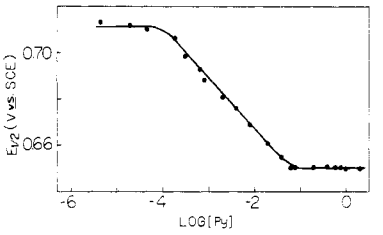

Figure 5. Plot illustrating shift of $E_{1/2}$ as a function of pyridine concentration for the first oxidation of 6×10^{-4} M (TPP)Hg in CH_2Cl_2–0.1 M TBAP.

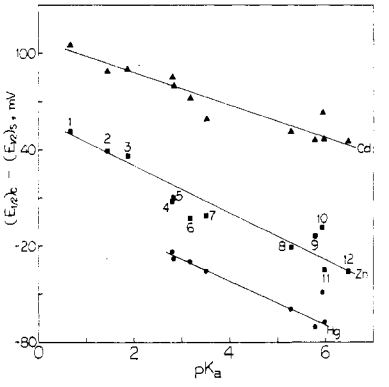

Figure 6. Plots illustrating potential shifts between the reactions (TPP)M/[(TPP)M]$^+$ and [(TPP)M(L)]/[(TPP)M(L)]$^+$ as a function of ligand pK_a: (▲) (TPP)Cd; (●) (TPP)Hg; (■) (TPP)Zn. $(E_{1/2})_s$ and $(E_{1/2})_c$ are defined by eq 4.

Cyclic voltammograms were measured for (TPP)Cd and (TPP)Hg in the presence and absence of each ligand in Table I. No change was observed in either the peak shape or current maximum of the current–voltage curves or in the measured half-wave potentials when the amount of ligand was less than 100th that of the porphyrin. Beyond this point, however, a shift of the oxidation peak occurred. For those complexes in which oxidations could be observed in the presence of complexing ligand (**1–12, 18**) the value of $E_{1/2}$ shifted at low ligand concentration from that of the uncomplexed form in a cathodic or anodic direction (depending upon the ligand) by between −140 and +70 mV. At higher concentrations of ligand, however, $E_{1/2}$ was invariant with further ligand additions. This shift of $E_{1/2}$ is illustrated by the typical plot of $E_{1/2}$ vs. log [py] shown in Figure 5. There is no significance to the slope of the line in the transition region between intermediate and high ligand concentrations. Similar plots were obtained for most ligands with (TPP)Hg and (TPP)Cd in this study, as well as with (TPP)Zn in a previous study.[1] The magnitude of the complete shift in half-wave potentials between (TPP)M and (TPP)M(L) is shown in Figure 6. In this figure, the difference $(E_{1/2})_c - (E_{1/2})_s$ is plotted vs. the ligand pK_a.

In the presence of higher concentrations of nitrogenous bases, the potential separation between the cathodic and anodic peaks increased with the amount of ligand such that $E_{pa} - E_{pc}$ became greater than the theoretical 60 mV for a one-electron diffusion-controlled reaction. At the same time, however, i_{pa}/i_{pc} remained constant, suggesting a reduction in the het-

Table IV. Half-Wave Potentials for the First Oxidation of (TPP)M(L) in CH_2Cl_2 Containing 0.1 M TBAP and 1.0 M Ligand

	$E_{1/2}$, V vs. SCE		
ligand[a]	(TPP)Zn(L)[b]	(TPP)Cd(L)	(TPP)Hg(L)
neat CH_2Cl_2	0.78[c]	0.64[c]	0.71[c]
1	0.83	0.74	0.71[e]
2	0.82	0.73	0.71[e]
3	0.82	0.73	0.71[e]
4	0.79	0.72	0.69
5	0.79	0.72	0.68
6	0.78	0.71	0.68
7	0.78	0.70	0.67
8	0.76	0.69	0.65
9	0.77	0.68	0.64
10	0.77	0.70	0.66
11	0.74	0.68	0.64
12	0.74	0.68	*d*
18	*d*	0.63	0.57

[a] The ligand number is identified in Table I. [b] Taken from ref 1. [c] Electrooxidation is of uncomplexed (TPP)M in neat CH_2Cl_2. [d] Reaction was not observable within the solvent range. [e] Due to small stability constants of (TPP)Hg and $[(TPP)Hg]^+$ with these ligands, the electrode reaction most likely involves the uncomplexed species.

Table V. Stability Constants (log $\beta_1{}^+$) for Axial Ligand Addition of Nitrogenous Bases to $[(TPP)M]^+$ in CH_2Cl_2 Containing 0.1 M TBAP[a]

	complex		
ligand[b]	$[(TPP)Zn(L)]^+$[c]	$[(TPP)Cd(L)]^+$	$[(TPP)Hg(L)]^+$
1	1.64	*d*	*d*
2	2.04	0.47	*d*
3	2.23	0.68	*d*
4	2.85	1.00	0.83
5	2.87	1.17	0.98
6	3.14	1.46	1.10
7	3.25	1.89	1.35
8	3.98	2.51	2.47
9	4.00	2.76	2.87
10	2.10	2.55	2.59
11	4.41	2.92	2.89
12	4.59	3.09	
18		5.13	5.18

[a] Reaction: $[(TPP)M]^+ + L \rightleftarrows [(TPP)M(L)]^+$. [b] Ligand number refers to Table I. [c] Data taken from ref 1. [d] Stability constant less than 0.25.

erogeneous electron-transfer rate constant upon complexation. No indication of nonreversibility was found during the time scale of the measurement.

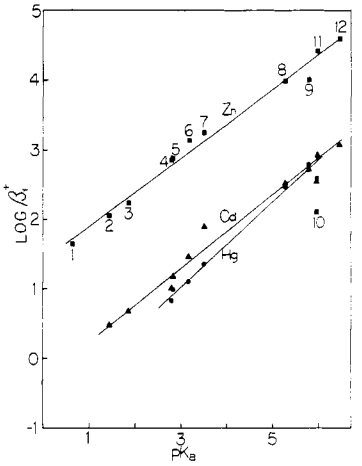

Figure 7. log $\beta_1{}^0$ vs. ligand pK_a for $[(TPP)M(L)]^+$, where M = Zn (■), Cd (▲), and Hg (●).

On the basis of analysis of the current–voltage curves as well as a knowledge of the ligand-binding properties of the neutral species, reactions 6 and 7 can be used to explain the overall

$$(TPP)M \overset{-e^-}{\rightleftharpoons} [(TPP)M]^+ \quad (6)$$

$$(TPP)M(L) \overset{-e^-}{\rightleftharpoons} [(TPP)M(L)]^+ \quad (7)$$

oxidation processes. At low ligand concentrations (TPP)M remains uncomplexed by a nitrogenous base and the electrode reaction proceeds as described by reaction 6. At high ligand concentrations (TPP)M(L) is formed in solution and this is reversibly oxidized to $[(TPP)M(L)]^+$ according to reaction 7.

Half-wave potentials for the electrochemical oxidation of (TPP)M(L) in CH_2Cl_2 containing 1 M ligand are presented in Table IV. Only 13 ligands were investigated due to the limited anodic oxidation range of several ligands. At 1 M ligand, electrooxidation is via the electron-transfer pathway of reaction 7.

Stability constants for addition of each nitrogenous base to the cation radical were calculated by using eq 4 and the data in Table IV, as well as the plots of $E_{1/2}$ vs. log [L]. These values are summarized in Table V. The correlations of log $\beta_1{}^+$ with the ligand pK_a are shown in Figure 7, and the linear regression fit according to eq 5 are given in Table II. The goodness of the fit indicates the interaction between $[(TPP)M]^+$ and nitrogenous bases is dominated by σ-bond strength similar to the reactions of TPPM with the same bases.

Table VI. Half-Wave Potentials for the First Oxidation of (TPP)M in Selected Solvents Containing 0.1 M TBAP

		$E_{1/2}$, V vs. SCE			$E_{1/2} - E_{1/2}(Fc)$,[d] V		
solvent[a]	DN[b]	(TPP)Zn	(TPP)Cd	(TPP)Hg	(TPP)Zn	(TPP)Cd	(TPP)Hg
$EtCl_2$	0.0	0.80	0.66	*c*	0.31	0.18	
CH_2Cl_2	0.0	0.78	0.64	0.71	0.29	0.14	0.22
CH_3NO_2	2.7	0.66	*c*	*c*	0.32		
PhCN	11.9	0.80	0.72	0.72	0.34	0.26	0.25
CH_3CN	14.1	0.77	0.72	*c*	0.38	0.32	
PrCN	16.6	0.83	0.77	*c*	0.36	0.31	
$(CH_3)_2CO$	17.0	0.87	0.87	*c*	0.38	0.36	
THF	20.0	1.02	0.87	0.84	0.35	0.21	0.18
DMF	26.6	0.86	0.72	*c*	0.38	0.24	
DMA	27.8	0.91	0.78	0.78	0.40	0.27	0.28
Me_2SO	29.8	0.87	*c*	*c*	0.42		
py	33.1	0.84	*c*	*c*	0.32		

[a] Abbreviations: $EtCl_2$, 1,2-dichloroethane; PhCN, benzonitrile; PrCN, *n*-butyronitrile; THF, tetrahydrofuran; DMF, dimethylformamide; DMA, *N*-dimethylacetamide; Me_2SO, dimethyl sulfoxide; py, pyridine. [b] Gutmann, V. "The Donor-Acceptor Approach to Molecular Interactions"; Plenum Press: New York, 1978; p 20. [c] Reaction not observable within solvent range. [d] Difference between measured couple and ferrocene/ferrocenium couple in the same solvent.

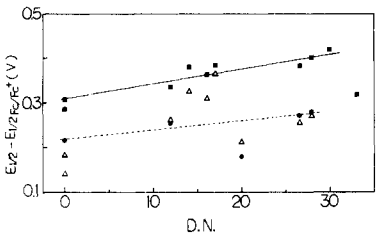

Figure 8. Plots showing solvent effect on $E_{1/2}$ for the first oxidation of (TPP)Cd (▲), (TPP)Hg (●), and (TPP)Zn (■).

Finally, the solvent effect on half-wave potentials was investigated. Half-wave potentials for each complex of (TPP)M were investigated in 12 nonaqueous solvents. Oxidation potentials are presented in Table VI, and a plot of $E_{1/2}$ vs. Gutmann DN is given in Figure 8.

Discussion

Ligand Addition to (TPP)M and Correlations with Ligand Properties. All of the ligands investigated in this study formed only 1/1 complexes with (TPP)Hg and (TPP)Cd, in agreement with similar results for (TPP)Zn.[1,11-13,15,16] There have been several reports that (TPP)M, where M = Zn, Cd, or Hg, may form six-coordinate complexes with donors other than nitrogen. (TPP)Zn was initially described as the six-coordinate complex $(TPP)Zn(H_2O)_2$,[30] but Hoard and co-workers later reinterpreted this species as a monoaquo derivative.[31] Recently Scherz and Levanon described a dimerization equilibrium for (TPP)Zn,[32] but Koehorst et al. pointed out that this seems unlikely.[33] (TPP)Cd initially appeared to form a six-coordinate complex with dioxane, but the apparent axial binding has been shown to have only weak solvent–metal interaction on the basis of the Cd–O bond distances (2.65 and 2.80 Å).[21] (TPP)Cd·2(dioxane) is thus best described as a four-coordinate complex. A dimer, $TPP((AcO)Hg)_2$, has been found for (TPP)Hg, but this compound easily collapses to the monomer upon treatment with a solvent mixture.[34]

On the basis of the data available, it now seems unlikely that (TPP)Cd or (TPP)Hg forms six-coordinate complexes. This conclusion is especially reinforced by the large size of the Cd and Hg cations (1.09- and 1.10-Å radii, respectively), which are forced to lie outside the plane of the porphyrin ring. In contrast, however, ionic size effects alone cannot rule out the possibility of forming octahedral complexes with (TPP)Zn, especially when these complexes are compared with those that are known to form with (TPP)Mg.[10,35] Both Zn(II) and Mg(II) have closed d-shell configurations with comparable ionic radii (0.86 Å for Mg^{II} and 0.88 Å for Zn^{II}), yet (TPP)Mg can form both 1/1 and 1/2 complexes with all of the nitrogenous bases in Table I.[29]

There is no electron population in the $d_{x^2-y^2}$ orbital of Mg(II) (whose lobes point directly toward the pyrrole nitrogens), and this allows Mg(II) to be squeezed into the hole of porphyrin plane to form a six-coordinate complex. It should be noted, however, that the second axial addition is not a favorable step as indicated by small values of K_2.[29] By comparison, if Zn(II) is squeezed into the porphyrin plane, its filled $d_{x^2-y^2}$ orbital will no longer overlap with the porphyrin π^* system, and there will be zero bond order for the bonding between Zn(II) and pyrrole nitrogens of TPP. This loss of bonding should, and does, prevent (TPP)Zn from forming a six-coordinate complex with nitrogenous bases.

Several conclusions may be drawn from the data in Table I. The first is that, within experimental error, there is no difference between the values presented in earlier studies for ligands **3**, **8**, **9**, **11**, and **14** and those that we have calculated in the present investigation. This is true despite the difference of ionic strength between this work and the earlier studies as well as the difference in method of calculation. The second observation is that for all three series of complexes the magnitude of log β_1^0 increases directly as a function of the pK_a of the donor ligand. This is true for both pyridines and imidazoles as axial ligands. This was shown earlier for the substituted pyridines[11,12] but not for the imidazoles. It is important to note that ligands **10** and **13** have been classified as sterically hindered ligands[12] and show substantially decreased values of binding constants with (TPP)Zn. The value of log β_1^0 is not reduced, however, for complexation of the same donor ligands with (TPP)Cd and (TPP)Hg, and these same ligands fit nicely on the plot of log β_1^0 vs. pK_a shown in Figure 1.

The increase of log β_1^0 with the ligand pK_a indicates that reaction 1 is dominated by the ligand to metal σ bonding. This increasing trend is understandable, for the donicity of the ligand increases with its pK_a. The polarizability of a specific donor is determined by the electronegativity of the coordinating site as well as the properties of neighboring groups within the donor molecule.[36] The less electronegative the coordinating site, the more polarizable it is. With an increase in ligand pK_a, more electron density will be placed on the pyridine nitrogen, making it more polarizable.

In addition to the correlation of log β_1^0 with the ligand pK_a, log β_1^0 can also be plotted vs. Hammett σ constants in the form

$$-\log (\beta_1/\beta_1^0) = \rho\sigma \qquad (8)$$

where β_1 represents stability constants for addition of one of the substituted pyridines to (TPP)M, β_1^0 is the stability constant for the (TPP)M(py) complex (the unsubstituted ligand), σ is the Hammett substituent constant for the meta or para substituent, and ρ is the reaction constant, which tells the magnitude of the effect of σ on the given reaction. (In this case the reaction is ligand addition given by eq 1.)

Linear correlations were obtained by plotting log (β_1/β_1^0) vs. σ for reactions of (TPP)Hg and (TPP)Cd similar to those described in ref 11, and a positive ρ was calculated from all plots. This positive value of ρ not only indicates that reaction 1 is dominated by σ bonding but also shows that Hg(II) is the best σ polarizer among these three metal ions. This conclusion is also obtained when one considers the value of a for each series of complexes, which is given in Table II.

Similar correlations between stability constants for (TPP)M(L) formation and the physical properties of the uncomplexed ligand have also been seen in the literature.[37,38] In a ^{15}N NMR study of ligand binding to (TPP)Zn, Gust and Neal found that ^{15}N chemical shifts ($\Delta\delta$) were correlated with electron-donating ability of the ligands.[37] A downfield shift of the porphyrin ^{15}N resonance resulted from the complexation of (TPP)Zn with substituted pyridines. As the substituent group became more electron releasing, $\Delta\delta$ became more negative in magnitude. Dominguez and co-workers also used the technique of NMR to study the metal–ligand interaction

(30) Fleischer, E. B.; Miller, C. K.; Webb, L. E. *J. Am. Chem. Soc.* **1964**, *86*, 2342.
(31) Glick, M. D.; Cohen, G. H.; Hoard, J. L. *J. Am. Chem. Soc.* **1967**, *89*, 1996.
(32) Scherz, A.; Levanon, H. *J. Phys. Chem.* **1980**, *84*, 324.
(33) Koehorst, R. B. M.; et al. *J. Chem. Soc., Perkin Trans. 2* **1981**, *77*, 1005.
(34) Hudson, M. F.; Smith, K. M. *Tetrahedron Lett.* **1974**, 2223.
(35) Storm, C. B.; Corwin, A. H.; Arellano, R. R.; Martz, M.; Weintraub, R. *J. Am. Chem. Soc.* **1966**, *88*, 2525.
(36) Ahrland, S. *Struct. Bonding (Berlin)* **1966**, *1*, 207.
(37) Gust, D.; Neal, D. N. *J. Chem. Soc., Chem. Commun.* 1978, 681.
(38) Dominguez, D. D.; King, M. M.; Yeh, H. J. C. *J. Magn. Reson.* **1978**, *32*, 161.

in doubly labeled ^{111}CdTPP($^{15}N_4$).[38] They found that complexation of the cadmium porphyrin with substituted pyridines gave ^{111}Cd chemical shifts having higher shielding and ^{15}N chemical shifts in the opposite direction. Both shifts were linear functions of the ligand pK_a.

Spectroscopic Properties of (TPP)M(L) and Correlation with Ligand Properties. Table III lists the absorption maxima and molar absorptivities of (TPP)Zn, (TPP)Cd, and (TPP)Hg complexed by 20 different nitrogenous bases. As seen from this table, large bathochromic shifts are observed upon going from (TPP)M to (TPP)M(L), with the magnitude of the shift being dependent upon the magnitude of the metal–ligand interaction.

The following observations may be made from the data in this table: (i) absorption maxima for all peaks shift gradually to longer wavelengths with an increase in ligand pK_a; (ii) the α and β bands have larger red shifts than those of the Soret band; (iii) ϵ shows an approximate positive correlation with the ligand basicity; and (iv) the ratio of α and β band intensities $\epsilon_\alpha/\epsilon_\beta$, varies from ligand to ligand.

Numerous correlations have been made in the literature between the spectroscopic properties of (TPP)Zn(L) and properties of the ligand.[13,16,39-41] These include correlations with Gutmann donor numbers of the ligand, pK_a of the ligand, dielectric constant functions of the donor ligand, or the Drago parameters E_B and C_B. In most cases with a given closely related set of ligands, linear relationships are obtained. As the ligand set is expanded, however, deviations begin to occur depending on the parameter selected.

One of the initial correlations by Cole et al.[16] involved the Soret red shift and the pK_a of the ligand. In this study separate relationships were obtained for a small series of pyridines and anilines. A later correlation by Vogel and Stalbush[40] involved plots of $-\Delta H$ (calculated from E and C parameters) with the Soret red shift of the (TPP)Zn(L) complex. Drago et al.[41] also used E and C parameters to analyze the correlation between ligand donor numbers and the Soret band shifts of (TPP)Zn adducts with various oxygen and nitrogen donor ligands. The authors pointed out that their approach with E and C parameters gave the best indication of σ-bond strengths and that all other relationships gave invalid measures of this effect.

On the other hand, Nappa and Valentine[13] found no such correlation between the red shift of the Soret band and $-\Delta H$ and concluded that, in general, for the addition of ligands to (TPP)Zn, a red shift cannot be correlated with $-\Delta H$. They did point out, however, that the red shift of the α band could be related to the ratio $\epsilon_\alpha/\epsilon_\beta$ and that ratio in turn was directly related to the amount of electron density on the metal.

In this study we have examined a number of correlations between spectral shifts or ratios of intensity of the α and β bands and separate empirical parameters related to bond strength, ligand polarity, or ligand base strength. As expected, linear correlations were most often obtained when we considered only the closely related substituted pyridines bound to (TPP)Zn. Inclusion of the imidazoles with the pyridine ligands added either scatter or curvature to the plots.

Examples of two investigated relationships are shown in Figures 3 and 4. The first is that of $\epsilon_\alpha/\epsilon_\beta$ vs. the position of the α band in cm^{-1}. This plot is presented for the spectra of (TPP)Zn(L), (TPP)Cd(L), and (TPP)Hg(L) and was selected for comparison with a similar linear plot constructed by Nappa and Valentine for (TPP)Zn(L) with a variety of ligands.[13] As seen from our data, a curvilinear relationship is observed for the reactions of Zn and almost no relationship is observed for Cd and Hg. However, when all three species are considered together, a good correlation is observed between the ratio $\epsilon_\alpha/\epsilon_\beta$ and ν_α.

Much better fits are obtained with correlations between log β_1^0 for ligand addition to (TPP)Zn and $\epsilon_\alpha/\epsilon_\beta$ of the (TPP)Zn(L) complex. This is shown in Figure 4. When only pyridines are considered, a linear relationship is observed for (TPP)Zn. This would suggest that, for a given series of ligands, the change of $\epsilon_\alpha/\epsilon_\beta$ can be related to the change of the metal–ligand bond strength. It should be noted that, since log β_1^0 is linearly related to the ligand pK_a (Figure 1), $\epsilon_\alpha/\epsilon_\beta$ also fits a linear plot for (TPP)Zn(L). Again, however, no well-defined trend emerges for (TPP)Cd(L) and (TPP)Hg(L).

It is interesting to note that there is almost no change in the ratio of molar absorptivities for (TPP)Cd(L) complexes despite large variations in log β_1. Likewise, for the complexation of (TPP)Hg(L) little difference exists in the spectral positions or intensities of the complex despite a change of 5 orders of magnitude in the stability constant of the complex. This may be related to the large out-of-plane displacement of the metal such that the metal–ligand bond strength has little effect on the spectra of the overall complex.

Electrode Reactions of (TPP)M and (TPP)M(L). In CH_2Cl_2 containing 0.1 M TBAP, half-wave potentials for the first oxidation of (TPP)Zn, (TPP)Cd, and (TPP)Hg were 0.78, 0.64, and 0.71 V, respectively. Potentials for the first two agree with the order that might be predicted from the central metal electronegativity[42] while that for (TPP)Hg is more anodic than expected. No such deviation is observed for metal phthalocyanines where complexes containing the more positive central metal ions are more difficult to oxidize.[43]

Kampas et al. found that the quantum yields of triplet-state formation paralleled the ease of oxidation for a large number of (TPP)M and (OEP)M complexes in nonaqueous solvents.[44] Although (TPP)Zn and (TPP)Cd fit the relationship between quantum yield and half-wave potential, the $E_{1/2}$ of (TPP)Hg was not included in this series.

Complexation of (TPP)Cd or (TPP)Hg with nitrogenous bases gave only small shifts of oxidation potential as shown by the data in Table IV. For (TPP)Hg(L) the maximum deviation in half-wave potentials was 70 mV for all but compound **18** while with (TPP)Cd(L), half-wave potentials shifted by only a maximum of 90 mV with respect to the uncomplexed (TPP)Cd. These shifts of $E_{1/2}$ are shown in Figure 6 for all three complexes and are small only because of the fact that stability constants of similar magnitudes are obtained for the oxidized and reduced forms of the complex. For other porphyrin complexes such as (TPP)Co and (TPP)FeX, differences in stability constants for ligand binding to the oxidized and reduced forms of the complex may vary by over 12 orders of magnitude[4,5,45] and up to 500-mV shifts in potential are observed between the complexed and the uncomplexed forms of the porphyrin.[4,5,46] Other porphyrin complexes, however, such as those containing Mn(III) and Mn(II) have formation constants virtually identical with those of most axially complexed ligands, and little change in $E_{1/2}$ is observed.[8]

Ligand Addition to [(TPP)M]$^+$ and Correlations with Ligand Properties. Stability constants for complexation of [(TPP)M]$^+$ with 20 nitrogenous bases are shown in Table V and plotted vs. the ligand pK_a in Figure 7. As seen from Table V and

(39) Kolling, O. W. *Inorg. Chem.*, **1979**, *18*, 1175.
(40) Vogel, G. C.; Stahlbush, J. R. *Inorg. Chem.* **1977**, *16*, 950.
(41) Drago, R. S.; Kroeger, M. K.; Stahlbush, J. R. *Inorg. Chem.* **1981**, *20*, 306.
(42) Fuhrhop, J. H.; Kadish, K. M.; Davis, D. G. *J. Am. Chem. Soc.* **1973**, *95*, 5140.
(43) Lever, A. B. P.; Minor, P. C. *Inorg. Chem.* **1981**, *20*, 4015.
(44) Kampas, F. J.; Yamashita, K.; Fajer, J. *Nature (London)* **1980**, *284*, 40.
(45) Bottomley, L. A.; Kadish, K. M. *Inorg. Chem.* **1981**, *20*, 1348.
(46) Walker, F. A.; Kadish, K. M.; Beroiz, D. *J. Am. Chem. Soc.* **1976**, *94*, 3484.

Figure 7, the magnitude of log β_1^+ for a given set of ligands follows the order Zn > Cd ≈ Hg. After losing one π electron, the central metal ion in $[(TPP)M]^+$ should become more electron deficient. As seen in Table II, a values for β_1^+ increase by 1.3–2.1 times compared to those for β_1^0. From this point of view nitrogen donors should show a larger stabilization effect on $[(TPP)M]^+$ than on (TPP)M. If this were the case, we would expect to see an absolute cathodic shift of $E_{1/2}$ from the uncomplexed form of (TPP)M upon adding ligands. This is not generally observed for ligands of low pK_a but does occur with ligands of higher pK_a as seen in Table IV and Figure 6. As seen from Table IV, a cathodic shift of potential from $(TPP)M/[(TPP)M]^+$ is seen for (TPP)Zn beginning with ligand **8**, for (TPP)Hg with ligand **4**, but for (TPP)Cd only with ligand **18**. The fact that ligands with lower pK_a bind the lower oxidation state of (TPP)M more strongly than the higher state leads to a positive shift in $E_{1/2}$ for a comparison with two individual couples. Similar crossovers of ligand-binding strengths for the oxidized and reduced forms of the complex have been observed for the electrode reactions of $(TPP)Fe(L)_2^+/(TPP)Fe(L)_2$[9] and $(TPP)Ru(CO)(L)^+/(TPP)Ru(CO)(L)$[47] with the same ligands as in this present study. Finally, when considering all of the ligands, one does see the expected negative shift of $(E_{1/2})_c - (E_{1/2})_s$ with increased pK_a.

Solvent Effects on Half-Wave Potentials. Half-wave potentials for the first oxidation of (TPP)M in 12 different nonaqueous solvents are shown in Table VI. Values are presented both as the experimentally measured value vs. SCE and after correction for liquid-junction potential (as $E_{1/2}$ vs. the ferrocene/ferrocenium couple in each solvent). This latter value allows for the examination of thermodynamic relations between half-wave potentials in different nonaqueous solvents and the binding ability of the solvent.

In an earlier publication, plots of $E_{1/2}$ for $(TPP)Zn/[(TPP)Zn]^+$ (referenced against the ferrocene/ferrocenium couple) vs. Gutmann DN gave a positive correlation.[3] A similar correlation is observed for the electrode reactions of (TPP)Hg as seen in Figure 8. Although the solvent data for (TPP)Hg are limited (due to small solubility in most solvents), there appears to be a slightly positive shift of $E_{1/2}$ as a function of solvent DN. When THF (which rarely seems to fit $E_{1/2}$–DN relationships) is excluded, the magnitude of the shift amounts of only 60 mV on changing from the nonbonding solvent CH_2Cl_2 to the more strongly bonding solvent DMA.

This lack of sensitivity of $E_{1/2}$ to DN of the solvent may be due, in part, to the fact that the solvents utilized are only weakly coordinated to (TPP)Hg. For example, the stability constant for binding to (TPP)Hg by pyridine (the solvent of highest DN) gives a log β_1^0 of 1.45 (see Table I). A decreased value of log β_1^0 = 0.46 was obtained for complexation by DMA under the same experimental conditions. This is the strongest bonding neat solvent in which oxidations could be obtained and yet only weak binding is observed.

(47) Kadish, K. M.; Leggett, D. J.; Chang, D. *Inorg. Chem.*, companion paper in this issue.

Finally, as seen in Figure 8 and Table VI, (TPP)Cd shows a large scatter in the data of $E_{1/2}$ vs. DN. Drago et al.[41] have suggested that there should be deviations in a plot of Gutmann DN vs. any measured property related to σ-bond strength. They found that solvents which were weak adducts (DN < 22) all had positive deviations from the best fit values and that solvents which acted as strong adducts (DN > 25) all had negative deviations. Generally, a large deviation implies dominance by some other effect. Because Cd(II) lies further out of the porphyrin plane than Zn(II), there can be greater solvation for Cd(II). This large dipole–dipole interaction may be the factor responsible for the large scatter of the data in plots of $E_{1/2}$ with DN.

Conclusions

In summary, we have presented the first thermodynamic data for reactions of the π cation radicals $[(TPP)Hg]^+$ and $[(TPP)Cd]^+$ with nitrogen donor ligands. We have also significantly extended the amount of data available for the simple ligand addition reactions of (TPP)Cd and (TPP)Hg in nonaqueous media. A combination of data for these neutral *and* positively charged five-coordinate complexes with electrooxidation potentials for the reactions $(TPP)M/[(TPP)M]^+$ should aid us in future interpretations of electrochemical processes involving metalloporphyrin π cation radicals.

Acknowledgment. The support of the National Science Foundation (Grant No. CHE-7921536) is gratefully acknowledged.

Registry No. (TPP)Cd(3,5-dichloropyridine), 82582-68-1; (TPP)Cd(3-cyanopyridine), 82582-69-2; (TPP)Cd(4-cyanopyridine), 27516-49-0; (TPP)Cd(3-chloropyridine), 82582-70-5; (TPP)Cd(3-bromopyridine), 82582-71-6; (TPP)Cd(3-acetylpyridine), 82582-72-7; (TPP)Cd(4-acetylpyridine), 82582-73-8; (TPP)Cd(pyridine), 27417-58-9; (TPP)Cd(3-picoline), 82582-74-9; (TPP)Cd(2-picoline), 82582-75-0; (TPP)Cd(4-picoline), 27516-48-9; (TPP)Cd(3,4-lutidine), 82582-76-1; (TPP)Cd(2-aminopyridine), 82582-77-2; (TPP)Cd(4-aminopyridine), 27417-57-8; (TPP)Cd(4-(*N*,*N*-dimethylamino)-pyridine), 82582-78-3; (TPP)Cd(piperidine), 82598-65-0; (TPP)-Cd(imidazole), 82582-79-4; (TPP)Cd(1-metrhylimidazole), 82582-80-7; (TPP)Cd(2-methylimidazole), 82582-81-8; (TPP)Cd(1,2-dimethylimidazole), 82582-82-9; (TPP)Hg(3,5-dichloropyridine), 82582-90-9; (TPP)Hg(3-cyanopyridine), 82582-91-0; (TPP)Hg(4-cyanopyridine), 27417-56-7; (TPP)Hg(3-chloropyridine), 82582-92-1; (TPP)Hg(3-bromopyridine), 82582-93-2; (TPP)Hg(3-acetylpyridine), 82582-94-3; (TPP)Hg(4-acetylpyridine), 82582-95-4; (TPP)Hg-(pyridine), 27417-55-6; (TPP)Hg(3-picoline), 27417-54-5; (TPP)-Hg(2-picoline), 82582-96-5; (TPP)Hg(4-picoline), 27417-53-4; (TPP)Hg(3,4-lutidine), 82582-97-6; (TPP)Hg(2-aminopyridine), 82582-98-7; (TPP)Hg(4-aminopyridine), 27516-50-3; (TPP)Hg(4-(*N*,*N*-dimethylamino)pyridine), 82582-99-8; (TPP)Hg(piperidine), 82598-66-1; (TPP)Hg(imidazole), 82583-00-4; (TPP)Hg(1-methylimidazole), 82583-01-5; (TPP)Hg(2-methylimidazole), 82583-02-6; (TPP)Hg(1,2-dimethylimidazole), 82583-03-7; (TPP)Cd, 14977-07-2; (TPP)Cd(PhCN), 82582-83-0; $(TPP)Cd(CH_3CN)$, 82582-84-1; (TPP)Cd(PrCN), 82582-85-2; $(TPP)Cd((CH_3)_2CO)$, 82582-86-3; (TPP)Cd(THF), 82582-87-4; (TPP)Cd(DMF), 82582-88-5; (TPP)Cd(DMA), 82582-89-6; (TPP)Hg, 24552-22-5; (TPP)-Hg(PhCN), 82583-04-8; (TPP)Hg(THF), 82583-05-9; (TPP)Hg-(DMA), 82583-06-0.